International Journal of Bioprinting

REVIEW ARTICLE

Application of 3D-bioprinted nanocellulose and cellulose derivative-based bio-inks in bone and cartilage tissue engineering

Lan Lin[1†], Songli Jiang[1†], Jun Yang[2], Jiandi Qiu[2], Xiaoyi Jiao[1], Xusong Yue[2], Xiurong Ke[2], Guojing Yang[2], Lei Zhang[1,2*]

[1]Department of Orthopaedic Surgery, The First Affiliated Hospital of Wenzhou Medical University, Wenzhou 325000, China

[2]Department of Adult Reconstruction, The Third Affiliated Hospital of Wenzhou Medical University, Wenzhou 325200, China

(This article belongs to the *Special Issue: 3D Printing in Tissue Engineering*)

Abstract

Three-dimensional (3D) printing is a modern, computer-aided, design-based technology that allows the layer-by-layer deposition of 3D structures. Bioprinting, a 3D printing technology, has attracted increasing attention because of its capacity to produce scaffolds for living cells with extreme precision. Along with the rapid development of 3D bioprinting technology, the innovation of bio-inks, which is recognized as the most challenging aspect of this technology, has demonstrated tremendous promise for tissue engineering and regenerative medicine. Cellulose is the most abundant polymer in nature. Various forms of cellulose, nanocellulose, and cellulose derivatives, including cellulose ethers and cellulose esters, are common bioprintable materials used to develop bio-inks in recent years, owing to their biocompatibility, biodegradability, low cost, and printability. Although various cellulose-based bio-inks have been investigated, the potential applications of nanocellulose and cellulose derivative-based bio-inks have not been fully explored. This review focuses on the physicochemical properties of nanocellulose and cellulose derivatives as well as the recent advances in bio-ink design for 3D bioprinting of bone and cartilage. In addition, the current advantages and disadvantages of these bio-inks and their prospects in 3D printing-based tissue engineering are comprehensively discussed. We hope to offer helpful information for the logical design of innovative cellulose-based materials for use in this sector in the future.

Keywords: 3D bioprinting; Nanocellulose; Cellulose derivative; Tissue engineering; Bio-ink; Bone

†These authors contribute equally to this work.

***Corresponding author:**
Lei Zhang (zhanglei@wmu.edu.cn)

Citation: Lin L, Jiang S, Yang J, *et al*., 2023, Application of 3D-bioprinted nanocellulose and cellulose derivative-based bio-inks in bone and cartilage tissue engineering. *Int J Bioprint*, 9(1): 637. https://doi.org/10.18063/ijb.v9i1.637

Received: July 29, 2022
Accepted: September 23, 2022
Published Online: November 9, 2022

1. Introduction

Three-dimensional (3D) printing allows the layer-by-layer deposition of 3D structures. Bioprinting, a 3D printing technology, has become widely used technique because of its capacity to establish scaffolds for living cells with extreme precision[1]. Owing to reproducibility, structural complexity, and high-precision control of the distribution of constituents such as cells, 3D-bioprinted scaffolds have received considerable attention

Table 1. Types, typical sizes, crystallinity and functions of nanocellulose

Type of nanocellulose	Typical size	Crystallinity	Mechanical strength	Characteristic
Nanofibrillated cellulose (NFC)	High aspect ratio; lengths: 0.5–2 μm; diameters: 5–60 nm	Contain both amorphous and crystalline regions; crystallinity about 60%	Tensile strength: 1 GPa, Young's modulus: 30 GPa	Good biocompatibility, biodegradability, water retention
Nanocrystalline cellulose (NCC)	High aspect ratio (~70); the smallest nanoscale dimensions of any nanocellulose; lengths: 0.05–0.5 μm; diameters: 3–5 nm	Crystallization zone only; highly crystalline (54–88%)	Tensile strength: 7.5 GPa, Young's modulus: 120 GPa	High mechanical strength, high crystallinity, good biocompatibility, biodegradability
Bacterial nanocellulose (BNC)	Lengths: several micrometers; diameters: 20–100 nm	Super high crystallinity (up to 95%)	Young's modulus up to 70 GPa	High water absorption, high air permeability, porous structure, good biocompatibility, biodegradability, high purity, simple purification process, expensive

in tissue engineering (TE)[2]. In addition, numerous studies have reported the use of 3D bioprinting in a wide range of TE applications, particularly in the fabrication of skin[3], heart[4], bone, and cartilage tissues[5]. At present, 3D bioprinting is a rather established technique, and can be categorized into several main methods: inkjet, extrusion, laser-assisted, and stereolithography methods[6]. However, bio-ink is the most important component, particularly in TE. Generally, several basic properties of bio-inks, including biocompatibility, printability, biodegradability, and mechanical properties, are taken into account in TE.

Cellulose, one of the most prevalent natural polymers, is a linear polymer comprising β-D-glucose. It is not only found in plants, but also in bacteria and algae. The hydrogen bond crosslink between β-D-glucose molecules makes cellulose rigid, and cellulose also has high biocompatibility as a natural polymer; therefore, cellulose, which is an abundant natural resource, is used to make bio-ink and claims an important place in the field of TE. Currently, nanocellulose and cellulose derivatives, which are the main forms of cellulose used in TE, are used as the main component of TE scaffolds and often as conditioning agents for other natural polymer inks (alginate [Alg] and gelatin).

The objective of this review is to present recent developments in 3D bioprinting using nanocellulose and cellulose derivatives in bone and cartilage TE that have been developed in the last five years. We also elaborate their potential applications in this emerging field.

2. Nanocellulose

Nanoscale cellulose derivatives are referred to as nanocellulose. Their intrinsic properties, including morphology, size, mechanical strength, and crystallinity, are determined by various sources and preparation methods. They are further divided into three categories: nanofibrillated cellulose (NFC), nanocrystalline cellulose (NCC), and bacterial nanocellulose (BNC) (Table 1). These intrinsic properties have led to their widespread use in the field of bone TE (Table 2).

2.1. NFC

2.1.1. Physicochemical properties and preparation of NFC

NFC is nanoscale cellulose obtained by degrading lignocellulosic biomass[7]. Owing to its nanoscale size, nanocellulose has good mechanical capabilities, strong cell adhesion, good biocompatibility, and water retention. NFC is composed of many entangled nanofibers that contain amorphous and crystalline regions[8]. NFC was previously prepared via high-pressure homogenization and grinding, and pretreatment is necessary to produce high-caliber NFC and reduce clogging and high-energy requirements in homogenizers. The most common pretreatment methods are enzymatic reactions[9] and 2,2,6,6-tetramethylpiperidine-1-oxyl free radical (TEMPO)-mediated oxidation[10], which weaken the interactions between plant cell walls. With a typical average length of approximately 0.5–2 μm, an average diameter of approximately 5–60 nm, a tensile strength of 1 GPa, and a modulus of 30 GPa, the size and strength of NFC are mostly dependent on the source and preparation technique. Moreover, many methods have been developed to modify the properties of NFCs. One of the examples is improving their hydrophilicity through physical adsorption and plasma discharge, which has led to their widespread use in various fields.

2.1.2. NFC 3D bioprinting in cartilage and bone repair

Owing to its remarkably high fidelity and biocompatibility, NFC bio-ink is a great material for 3D printing of TE scaffolds[11]. NFC is frequently used to modify the rheological characteristics of bio-inks and enhance their

Table 2. A summary of nanocellulose based bio-inks for 3D bioprinting applications in bone and cartilage TE

Bio-ink formulation	3D bioprinting method	3D bioprinting patterns	Bio-ink and scaffold properties	Effect on cell-loaded bio-ink	Ref.
NFC/Alg/poly (2-ethyl-2-oxazoline)	Extrusion-based 3D printing	3D-printed grids (20 × 20 × 0.4 mm^3)	• Increased ink viscosity • Shear thinning • Quick shear recovery • Increased mechanical strength	• Up to 90% cell activity after 21 days of cell encapsulation	[15]
NFC/Alg/polydopamine nanoparticles	Extrusion-based 3D printing	A grid structure (20 mm × 20 mm, 6 layers)	• Increase of ink viscosity • Shear thinning • Enhanced recovery rate • Increased mechanical strength	• Enhanced metabolic activities • Higher expression of osteogenesis-related genes	[22]
NCC/CS/HEC/glycerophosphate	Extrusion-based 3D printing	Solid cylindrical scaffolds (8 mm diameter × 2 mm thickness)	• Increased ink viscosity • Increased mechanical strength	• Higher expression of osteogenic markers • Enhanced mineral deposition • Enhanced ALP activity	[31]
Nanocellulose blends (NCB)	Extrusion-based 3D printing	Square grids (40 × 40 × 1.7 mm^3, a single layer)	• High-porosity structure • Higher stability and fidelity • Facilitates chondrocyte adhesion	• Maintenance of the round chondrogenic phenotype • Increased cell viability • Enhanced metabolic activities	[37]
Aqueous counter collision (ACC)-BNC	Extrusion-based 3D printing	A grid (5 × 5 × 1 mm^3)	• Outstanding printability • Mechanical stability • Structural integrity • High water-binding capacity	• Enhanced chondrocyte proliferation • Increased deposition of glycosaminoglycans	[51]
BNC/silk fibroin/gelatin	Extrusion-based 3D printing	Small grids (10 × 10 × 0.4 mm^3, 2 layers) / large grids (20 × 20 × 0.6 mm^3,15 layers)	• Increased print resolution • Enhanced mechanical properties • Improved pore connectivity	• Increased cell viability • Enhanced cell adhesion, proliferation, and differentiation	[52]

printability. Additionally, NFC is similar in size to collagen fibers, so NFC-based scaffolds have unique advantages in cartilage regeneration[12]. Given that chondrocytes exhibit high cell viability in Alg inks[13], their low ink viscosity limits their development in 3D bioprinting. Therefore, many researchers have mixed NFC with Alg to compensate for its low zero-shear viscosity for cartilage repair. Markstedt *et al.* prepared NFC-Alg bio-ink for cartilage TE[14] with high print resolution and fidelity, which combines the rheological characteristics of NFC with the crosslinking capabilities of Alg. Despite cell loss on scaffolds filled with human nasal chondrocytes (hNCs) as a result of shearing during printing, after 7 day of culture, the cell survival rate was considerably improved. Trachsel *et al.* created double network (DN) polymer hydrogels employing Alg and poly (2-ethyl-2-oxazoline) (PEOXA)[15]. DN usually consists of a primary covalent cross-linked network that provides elasticity and a secondary non-covalent cross-linked network that provides ductility; therefore, DN tends to have high strength[16]. PEOXA-Alg hydrogels can sequester living cells after enzymatic and ionic crosslinking to form DN. In addition, NFC can be added to the DN solution to enhance the viscosity and shear-thinning. With the addition of NFC, the viscosity of the ink increases, while the bio-ink displays quick shear recovery characteristics. This rapid shear recovery is also the reason why the NFC scaffold gives a high print resolution while maintaining the viability of the cells in the ink (avoiding shear damage). In addition to having 3D structures with high shape integrity after double crosslinking, the DN-NFC bio-ink-printed cartilage constructs loaded with human auricular chondrocytes (hACs) also showed up to 90% cell activity after 21 days of cell encapsulation. Therefore, we are aware that the NFC characteristics are not affected by these sophisticated multiple crosslinks.

The sulfated version of Alg has recently received increased attention because of its ability to bind a variety of growth factors and promote chondrocyte proliferation and collagen II deposition[17]. Müller *et al.* added NFC to alginate sulfate to increase the printability and mechanical strength of the bio-ink and bioprinted NFC-alginate sulfate bio-inks loaded with bovine chondrocytes[18]. As expected, the addition of NFC significantly improved the printability of alginate sulfate without affecting its osteogenic properties.

In clinically applicable *in vivo* investigations, NFC-Alg composite hydrogel scaffolds have shown remarkable cartilage-promoting characteristics. Apelgren *et al.* implanted 3D-bioprinted constructs (5 × 5 × 1.2 mm), which was prepared using three sets of NFC-Alg bio-inks loaded with hNCs, human bone marrow-derived

mesenchymal stem cells (hBMSCs), and a mixture of both, subcutaneously on the backs of nude mice[19]. The NFC aids in enhancing the ink's capacity to print in this situation as well. After 60 days, the explanted constructs all had significant levels of cellular activity, and from days 30 to 60, both hNCs and mixed groups displayed increased chondrogenesis and proliferation of glycosaminoglycan (GAG)-positive cells. This study demonstrated that NFC-based hydrogel scaffolds may exert their benefits in animal models while retaining cell viability; therefore, we anticipate their widespread clinical application in the future.

TEMPO-oxidized NFC (T-NFC) has a significant nucleation impact on hydroxyapatite due to the carboxylate groups acquired following its modification[20] and has been reported in conjunction with Alg for 3D printing in bone TE[21]. Im *et al*. used bio-ink obtained from Alg, T-NFC, and polydopamine nanoparticles (PDANPs) to obtain osteogenic structures via 3D bioprinting[22]. Compared to pure Alg gels, the recovery rate and compressive strength of the T-NFC-containing hydrogels were enhanced. More importantly, the expression of osteogenesis-related genes (alkaline phosphatase [*ALP*], *Runx2*, and *OPN*) was enhanced in composite 3D-bioprinted scaffolds loaded with MC3T3-E1 osteoblasts containing T-NFC and PDANPs, along with calcium production and deposition (biomineralization) on the scaffolds. Given its excellent printability, mechanical strength, and capacity to trigger osteogenesis, this T-NFC-containing bio-ink has great potential for use in bone TE. Interestingly, as a viscosity modifier for bio-inks, T-NFC not only increases the viscosity, but also reduces it when the ink viscosity is too high to prevent the restriction of cell activity and proliferation. Bioactive glass (BG) is frequently utilized in osteogenic bio-inks because of its excellent biocompatibility and ability to stimulate osteogenesis by forming a hydroxyapatite layer on its surface[23]. A BG-modified gelatin-Alg bio-ink for 3D bioprinting was developed by Ojansivu *et al*. However, after bioprinting, the high viscosity of the ink due to the inclusion of BG caused a sharp decline in the activity of the loaded cells[24]. After adjusting the ink viscosity by adding T-NFC, the hBMSCs in the printed scaffolds exhibited high activity and proliferative capacity without altering the osteogenic capabilities of BG. The fact that T-NFC interferes with crosslinking by competing with the Alg ink for cations produced by BG may be the cause of this viscosity-modulating action. Monfared *et al*. added Ca^{2+} as an ionic crosslinking agent to T-NCF, and the strong physical interaction with the carboxyl group of T-NCF was used as the first crosslink. In the case of water-soluble vitamin B as a photoinitiator, the poly (ethylene glycol) (PEG)-added ink was photo-crosslinked under blue light after 3D printing as the second crosslink[25]. By varying the T-NCF to Ca^{2+} ratio, the mechanical characteristics, stability, and fidelity of this double-crosslinked hydrogel scaffold may be modified. For instance, its hardness can be changed between 1 and 45 kPa. The carboxylic acid group in T-NFC can not only enhance the nucleation of hydroxyapatite to promote osteogenesis, but can also be used as a crosslinking target to adjust the rheological properties of the ink, and its functional diversity has greatly improved its applications in bone TE.

2.2. NCC

2.2.1. Physicochemical properties and preparation of NCC

NCC is the smallest of nanocellulose products, with a length of 0.05–0.5 μm and a diameter of 3–5 nm[26]. Compared with NFC, which contains amorphous regions, NCC contains only crystalline regions, which gives it a more rigid structure[7]. NCC is renowned for its high mechanical strength (~7,500 MPa), high aspect ratio (~70), amphiphilicity, and high crystallinity[27]. The preparation of NCC is more complex than that of NFC. Cellulose powder is first obtained by washing and mechanical grinding of lignocellulosic biomass, followed by purification via alkali treatment or acid-chlorite treatment to remove impurities, and finally, by acid hydrolysis to obtain NCC[28]. The crystalline portions that are acid-resistant are maintained during acid hydrolysis, whereas the non-crystalline parts are hydrolyzed because they are not acid-resistant. NCC preparation methods have a direct effect on both morphological traits and physical properties. For example, the enzymatic hydrolysis of NCC has better mechanical and heat properties than acid hydrolysis. The sphere-shaped NCC obtained via combined hydrochloric and sulfuric acid hydrolysis has greater heat resistance than the usual rod-shaped NCC[27].

NCC has various applications in medicine, including TE, medication delivery systems, and antibacterial agents. In bone TE, NCC can be used as an enhancer, additive, or biomaterial to enhance the mechanical and biocompatibility of scaffolds[29].

2.2.2. NCC 3D bioprinting in cartilage and bone repair

NCC promotes gelation of composite hydrogels through intermolecular hydrogen bonding to improve the mechanical properties of scaffolds for 3D bioprinting[30]. Maturavongsadit *et al*. prepared a bio-ink consisting of thermogelling chitosan (CS), NCC, β-glycerophosphate (BGP), and hydroxyethyl cellulose (HEC) to develop an optimal CS-NCC-based bio-ink for 3D bioprinting (Figure 1A and B)[31]. The ink is a heat-sensitive hydrogel with fast gelation caused by the formation of hydrogen bonds between CS and NCCs at 37°C (Figure 1C).

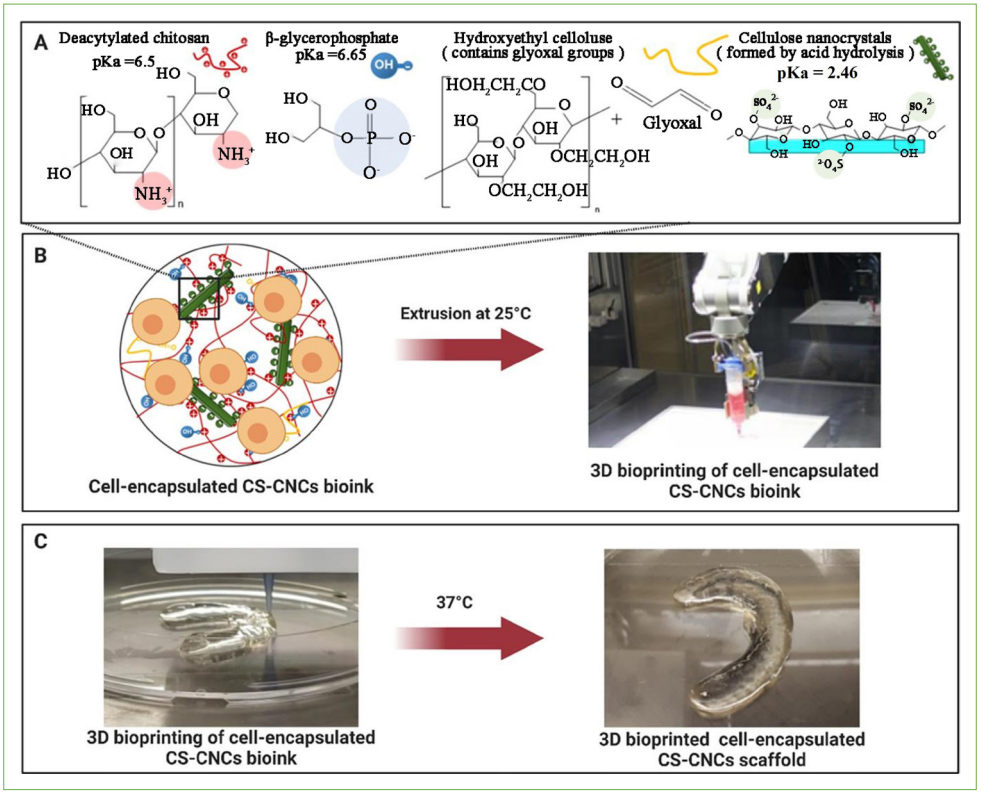

Figure 1. Schematic illustration of the 3D bioprinting process. (A) Bio-ink consisting of CS, NCC, BGP, and HEC. (B) Cell-loaded CS-NCCs bio-inks printed by 3D bioprinter. (C) Rapid gelation of 3D-bioprinted knee meniscus at 37°C[31]. Images reproduced with permission.

The inclusion of NCC also enhances viscosity, Young's modulus, yield stress, and energy storage modulus, which significantly enhances printing as well as mechanical properties of the scaffold. More significantly, because the addition of NCC causes ALP activity to peak by day 7, osteogenesis occurs more quickly in the NCC group than in the control group, with enhanced mineral deposition and elevated expression of osteogenic markers. This may be related to the enhanced mechanical properties of the scaffold[32].

Dutta *et al.* used 1% NCC/Alg/Gel+BMP2 bio-ink-printed scaffolds for *in vivo* studies using a rat CCD-1 calvarial defect model[33]. In contrast to the positive (BMP2-treated groups) and negative control groups, the 1% NCC/Alg/Gel+BMP2 group showed a significant increase in bone volume and reduction in bone defects. Additionally, no significant inflammatory response was observed at the implantation site, demonstrating the biocompatibility of NCC. However, the addition of NCC resulted in low swelling efficiency, indicating a reduction in the capacity to absorb water, which may be related to the improved crosslinking ability of the composite scaffold. Interestingly, Patel *et al.* also prepared NCC/Alg/Gel bio-ink at different concentrations, but the expansion efficiency of the obtained scaffolds was positively correlated with the concentration of NCC[34]. Nevertheless, the composite scaffolds prepared by the two investigators showed similar improvements in mineralization potential, osteogenic gene expression, mechanical strength, and cellular activity. Additionally, the authors discovered that an NCC concentration of 1% was ideal for the survival of hBMSCs and that cell activity declined with the increase in NCC concentration. Surface charge may be responsible for this phenomenon[35].

While commonly used techniques to obtain NCC and NFC bio-inks often have high costs and low recovery rates, a technology called American Value-Added Pulping (AVAP®) allows the preparation of NCC, NFC, and nanocellulose blends (NCB) at low cost[36]. Jessop *et al.* prepared a bio-ink loaded with human nasoseptal chondrocytes by mixing NCB obtained using the AVAP technique with Alg[37]. Compared to NCC-Alg and NFC-Alg, the NCB-Alg bio-ink has better stability and fidelity, which may be related to the greater entanglement between the hybrids. Under scanning electron microscopy (SEM), NCB-Alg has a superior high-porosity structure (Figure 2E and G) compared to 2.5% Alg bio-ink (Figure 2A and C), which facilitates chondrocyte adhesion while maintaining its round chondrogenic phenotype (Figure 2F and H), indicating that maintaining round

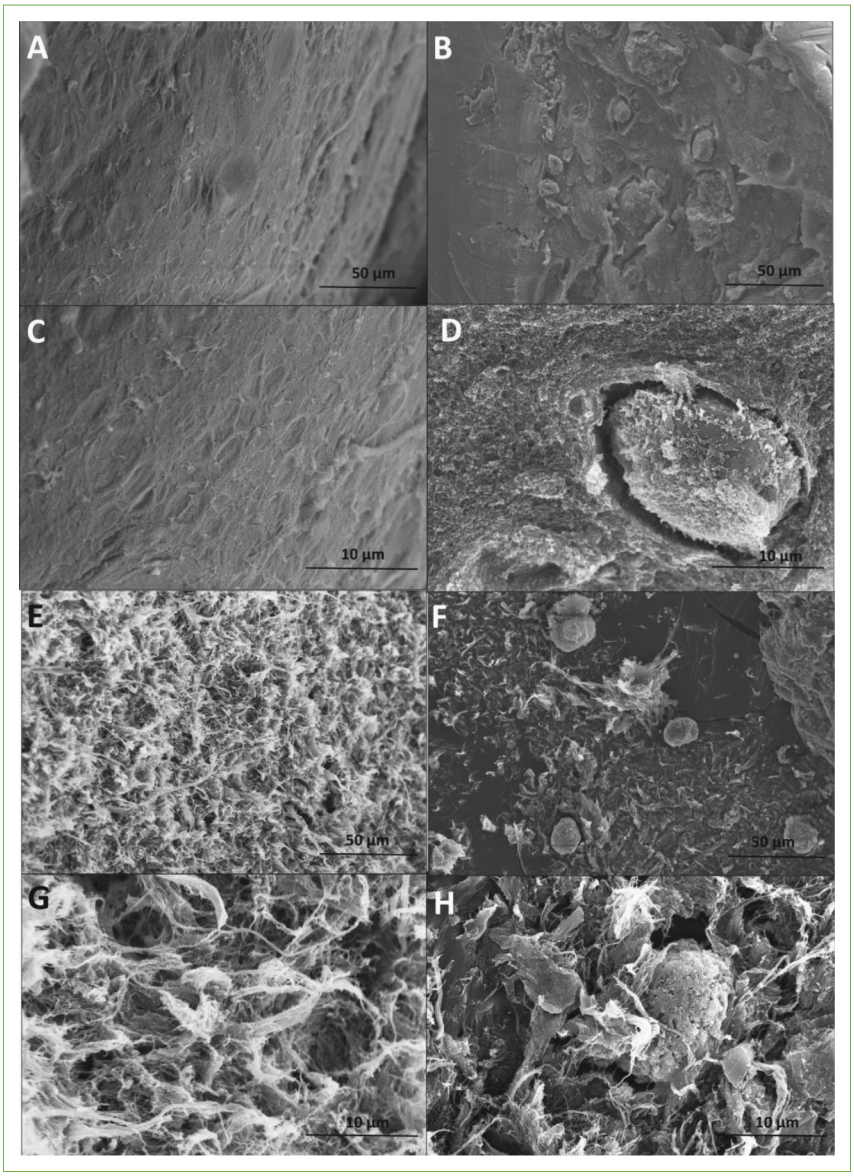

Figure 2. SEM after bioprinting of Alg and nanocellulose blends ink. (A and C) Alg bio-ink without cells. (B and D) Alg bio-ink loaded with human nasal septal chondrocytes after 3 weeks of culture. (E and G) NCB-Alg bio-ink without cells. (F and H) NCB-Alg bio-ink loaded with human nasal septal chondrocytes after 3 weeks of culture[37]. Images reproduced with permission.

cell morphology is a requirement for chondrogenesis[38]. This also indicated that NCB-Alg had a suitable nano-environment for chondrogenesis.

2.3. BNC

2.3.1. Physicochemical properties and preparation of BNC

The majority of cellulose is derived from plants. However, microorganisms are also an important source of cellulose, especially BNC. It is believed that bacterial cellulose is mainly synthesized to protect against ultraviolet radiation and enhance bacterial colonization while retaining moisture[39].

Unlike plant cellulose, BNC does not contain lignin or hemicellulose. Therefore, no complex steps, such as acidification and mechanical intervention, are required for purification, and only purification using the low energy consumption of sodium hydroxide (NaOH) solution is required. Moreover, BNC has a high-water content, up to 99%, unmatched by other biomaterials, as well as the ability to absorb water of more than 100 times its weight. Additionally, BNC has a nanofiber network that is similar to the extracellular matrix (ECM)[40], which has a significant impact on cell adhesion and migration. BNC is renowned for other qualities, including strong mechanical properties

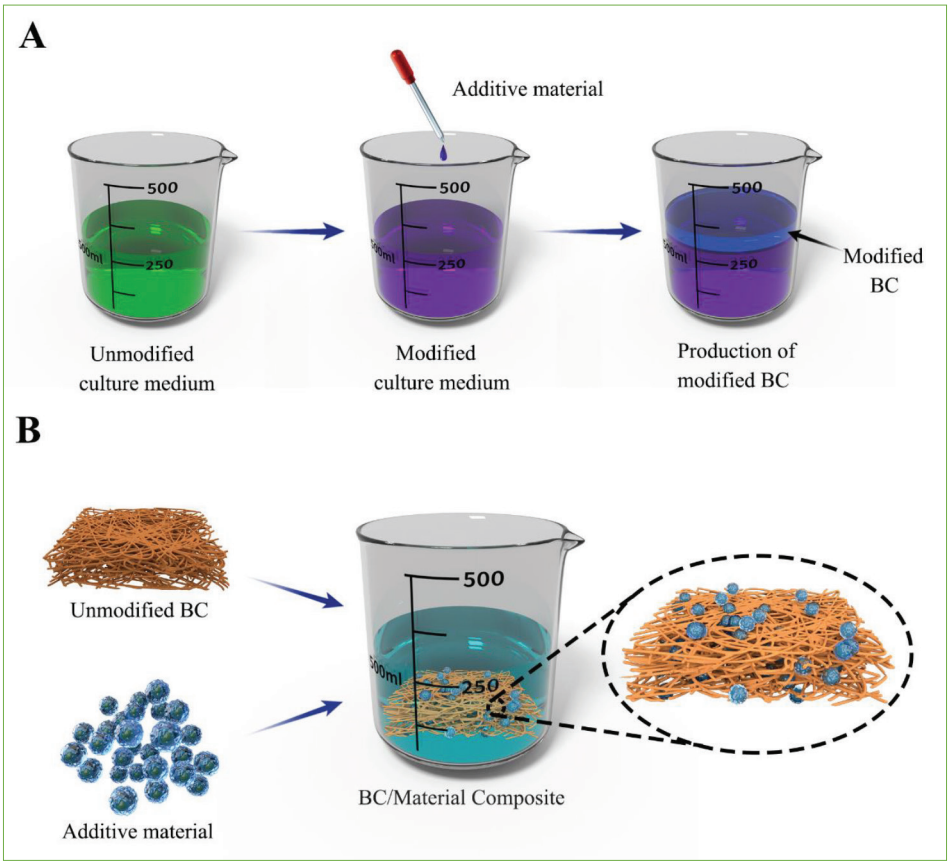

Figure 3. (A) *In situ* modifications: adding modified materials to the culture medium and changing the conditions of the medium. (B) *Ex situ* modifications: adding modified materials to the generated BC.

(Young's modulus up to 78 GPa), porous structure, and excellent biocompatibility[41]. Therefore, BNC has become a highly valued material for 3D printing in TE.

Different bacterial sources produce BNC with different properties. Among these, *Acetobacter xylinum* and *Gluconacetobacter xylinus* are the most widespread sources. *A. xylinum* can polymerize up to 200,000 glucose molecules per second via cellulose synthase[42]. Polymerized glucose chains are assembled from sub-elementary fibrils to microfibrils, and then further into tight ribbons. BNC are more expensive than other cellulose derivatives because of the high cost of the medium used to make BNC. However, numerous techniques, including strain mutagenesis, have been used to boost the production of synthetic cellulose from *A. xylinum*[43].

To optimize BNC for TE, different methods have been investigated to modify it, including *in situ* and *ex situ* modifications. *In situ* modification refers to changing the environment and conditions of bacterial culture (Figure 3A)[44]. Classical *in situ* modifications are often used to modulate the porosity of BNC scaffolds for bone TE. For example, Zaborowska *et al.* placed paraffin wax microspheres in a bacterial medium and made scaffolds after BNC generation, and then removed the paraffin wax microspheres to obtain bone scaffolds with large porosity[45]. *Ex situ* modifications refer to physical or chemical modifications after their formation (Figure 3B)[44]. Fang *et al.* used hydroxyapatite to modify the generated BNC to stimulate osteoblast proliferation and differentiation[46].

2.3.2. BNC 3D bioprinting in cartilage and bone repair

BNC is limited in 3D printing because of the complex protofibrous structure that causes it to frequently clog the nozzles of 3D printers and discourage cell migration[47]. Therefore, obtaining BNC dispersions is important for the preparation of BNC-based scaffolds. Given that TEMPO-oxidized NFC easily forms nanofibrous monomers in aqueous solutions, TEMPO-mediated oxidation is also widely used to decompose BNC and has been extensively investigated for the preparation of bone TE scaffolds. At present, maleic acid (MA) is considered an excellent reagent for the preparation of nanocellulose monomers[48]. Wang *et al.* obtained a dispersed BNC-gel composite ink by untwisting the tight protofibrous BNC network using MA and obtained a bone TE scaffold containing primary

MC3T3-E1 cells using 3D printing and implanted it into the skull defect of a Sprague-Dawley rat[49]. MA-treated scaffolds exhibited excellent mechanical properties and maintained MC3T3-E1 cell function. Kondo *et al.* invented a new technique for the decomposition of biomaterials into nanofibers using aqueous counter collision (ACC)[50]. ACC can effectively decompose BNC without chemical additives. Apelgren *et al.* used ACC to prepare a bacterial cellulose bio-ink containing hNCs, then used 3D bioprinting to prepare a bioprinted grid ($5 \times 5 \times 1$ mm^3), which was inserted into nude mice[51]. The skin graft was sutured to the scaffold to assess its biocompatibility. ACC-BNC bio-ink has high fidelity and viscosity than hydrolyzed BNC and has been used to print complex structures, such as biological auricles. Cartilage formation was observed in the biological network scaffold, as well as in the GAG deposition. After transplantation, the skin grafts revealed no adverse consequences, such as necrosis or inflammation, while the proliferation of chondrocytes was observed. This novel BNC bio-ink can also retain high biocompatibility in animal studies, paving the way for its clinical use.

Owing to its excellent mechanical properties and high fidelity, BNC is often used in addition to other bio-inks to modulate their properties. Huang *et al.* applied BNC to a silk fibroin (SF)/gelatin composite hydrogel scaffold to improve its mechanical properties and print resolution[52]. The scaffolds were also made macroporous and microporous via 3D printing and freeze-drying, respectively. The interconnected macropores and micropores promote cell adhesion, proliferation, and differentiation, as well as cartilage regeneration and cartilage-related gene expression[53]. The authors discovered that when the BNC concentration was increased, the scaffold displayed improved pore connectivity, cell content, and cell survival. Moreover, the authors demonstrated that the BCN-0.70 wt% bio-ink had the best print resolution and used it for the 3D printing of human meniscus models. Furthermore, the scaffold had a stable structure, and the BCN-0.70 wt% scaffold showed considerably reduced mass loss 1 month after subcutaneous implantation in nude mice compared to the control group.

3. Cellulose derivatives for 3D printing

The reaction of cellulose with chemical reagents can lead to different cellulose derivatives, the most common being cellulose ethers[54] and cellulose esters[55]. The hydroxyl group of cellulose is replaced with methyl, carboxymethyl, and acetate groups to produce cellulose derivatives. Cellulose derivatives have different properties because of their substitution by different groups. Some properties of the original component can be retained and result in unexpected interactions between the components in the final 3D product[56], which makes them a promising option for personalized medicine. Moreover, cellulose derivatives are widely used in 3D printing TE because of their low toxicity, biodegradability, and biocompatibility (Table 3).

3.1. Methylcellulose

3.1.1. Physicochemical properties and preparation of methylcellulose

Methylcellulose (MC) occupies an extremely important position among all cellulose derivatives. It is usually used as an additive in food and drugs because of its high biocompatibility[57]. MC is an ether cellulose derivative generated via the partial substitution of the three reactive hydroxyl groups of AGU (at C2, C3, and C6) in cellulose with methoxy groups. Unlike cellulose, which is insoluble in water, MC hydrogels have controlled solubility, which allows them to be widely employed in TE and regenerative medicine. The link between the structural domains generated by the hydrophilic hydroxyl groups and hydrophobic methoxy groups provides the foundation for the controllable solubility of MC. At low temperatures, the hydrophobic methoxy groups in MC interfere with the formation of hydrogen bonds between hydroxyl groups, allowing water molecules to enter the polysaccharide structure and electrostatically bind to the polar side chains, and subsequently forming hydrated layers around the methyl group (–OCH3) to reach a sol state[58]. When the temperature increases, the MC aqueous solution absorbs heat energy and the hydrogen bonds break down, resulting in intramolecular hydrophobic associations between MC molecules and the destruction of the hydrated layer. This is the basis for its use as a thermally reversible hydrogel[59]. Thermally reversible injectable MC hydrogels have been investigated for bone defect repair, using temperature changes to induce gelation, allowing the encapsulated cells to maintain their viability and stimulate osteogenesis[60]. The temperature at which the transition from sol to gel occurs for MC is defined as the lower critical solution temperature (LCST)[61]. LCST of MC hydrogels is particularly important because cell activity is highly temperature-dependent. The LCST of MC depends on a variety of variables, including concentration, degree of substitution (DS), molecular weight, sugar alcohols and anions. At the same time, the high viscosity of MC-based inks indicates good printability. It is generally accepted that 10% MC is suitable for printing, and the viscosity of MC is related to its concentration and temperature[62]. In addition, the viscosity of MC is susceptible to sterilization methods; γ-irradiation significantly reduces the viscosity and stability[63]. Owing to its properties, MC is widely used as a bio-ink for 3D bioprinting. It can be added to other

Table 3. A summary of recent studies on 3D printing of cellulose derivatives-based materials for bone and cartilage TE

Cellulose derivatives type	Ink composition	Cell lines	Bio-ink	Functions	Biomedical applications	Ref.
MC	MC/Alg/calcium phosphate cement (CPC)	Human chondrocytes (hCh)	Yes	• Increase of the ink viscosity	Bone and cartilage TE	[69]
MC	MC/Alg/plasma/calcium phosphate cement (CPC)	Mesenchymal stromal cells / primary osteoprogenitor cells	Yes	• Increase of the ink viscosity • Sacrificial ink	Bone TE	[70]
MC	MC/Alg/non-viral vector-pDNA complexes	Mesenchymal stromal cells	Yes	• Porogen • Increase of ink viscosity • Shear thinning	Bone and cartilage TE	[71]
CMC	CMC/glycol chitosan/ lactoferrin	MC3T3 cells/ bone marrow mesenchymal stem cells	Yes	• Improvement in the mechanical properties of the scaffold • Enhanced gel kinetics	Bio-ink preparation	[81]
CMC	CMC/gelatin/beta-tricalcium phosphate (β-TCP)	Primary stem cells from human exfoliated deciduous teeth	No	• Increase of ink viscosity • Maintenance of the scaffold's macroporosity	Bone TE	[85]
HPMC	HPMC/calcium magnesium phosphate	None	No	• Increase of the viscosity • Shear thinning	Bone TE	[89]
HPMC	HPMC-MA (hydroxy propyl methyl cellulose of methacrylation)/silk fibroin	Bone marrow mesenchymal stem cell	Yes	• Improvement in the mechanical properties of the scaffold • Enhanced gel kinetics	Cartilage TE	[90]
HEC	HEC/CNCs/glycerophosphate/CS	Pre-osteoblast cells (MC3T3-E1)	Yes	• Enhanced gel kinetics	Bone TE	[31]

inks to increase their printability and then removed by adjusting the LCST.

MC can be prepared in a variety of ways and is broadly classified into two types: homogeneous distribution[64] (a more regular distribution of methyl substituents along the chains) and heterogeneous distribution[65] (random distribution of the substituents). MC derivatives with DS between 1.3 and 2.5 are water soluble, while those with DS more than 2.5 are soluble in organic solvents[59].

3.1.2. MC 3D bioprinting in cartilage and bone repair

MC is applied in bone TE in three main aspects: (i) as a support ink, (ii) as a sacrificial ink, and (iii) to increase the viscosity of the blended bio-ink.

Given the low viscosity of Alg inks described earlier, MC plays a similar role to nanocellulose for printing high-fidelity scaffolds obtained by mixing with Alg[66]. Ahlfeld *et al.* proposed the use of a self-setting calcium phosphate cement (CPC) and Alg-MC bio-ink by multichannel 3D plotting to simulate a multilayered osteochondral tissue structure[67]. CPC is commonly accepted as the best bone replacement material because of its similarity to the mineral composition of bone and its *in vivo* conversion into calcium-deficient nanocrystalline hydroxyapatite (HAp), which is absorbed by osteoclasts for bone reconstruction[68]. To simulate the three-layer configuration of the osteochondral region, the uppermost layer consists of a human mesenchymal stem cells (MSCs)-laden Alg-MC fraction resembling the articular cartilage surface, the calcified cartilage region consists of a biphasic interwoven network of cell-laden Alg-MC and CPC, and the lowermost layer, the subchondral bone, consists of CPC. Between days 7 and 21, the cells remain highly active as they start to migrate aggressively from the Alg-MC to the CPC chain and exhibit an extended, elongated morphology[67]. Kilian *et al.* used human chondrocyte (hCh)-loaded Alg-MC ink together with CPC using 3D plotting to construct the osteochondral replacement scaffold described above (Figure 4A and B)[69]. A significant formation of cartilage ECM (i.e., sulfated glycosaminoglycans, collagen type II) on the scaffold was found[69].

Ahlfeld *et al.* developed an MC-based supportive hydrogel ink for 3D plotting to create clinically relevant geometries, including critical overhangs and cavities[62]. They designed MC as a support ink to co-print a human scaphoid bone model with CPC (Figure 4C) and used MC as a sacrificial ink to create the cavity[62]. As plasma contains a huge variety of angiogenic factors, in a recent study, CPC/plasma-Alg-MC was used to print a pre-vascularized bone tissue scaffold. The plasma-Alg-MC formed the lumen wall of the constructs, and CPC was used as an external scaffold (Figure 4D and E). Cells were found to cover the surface of the lumen after 35 days[70].

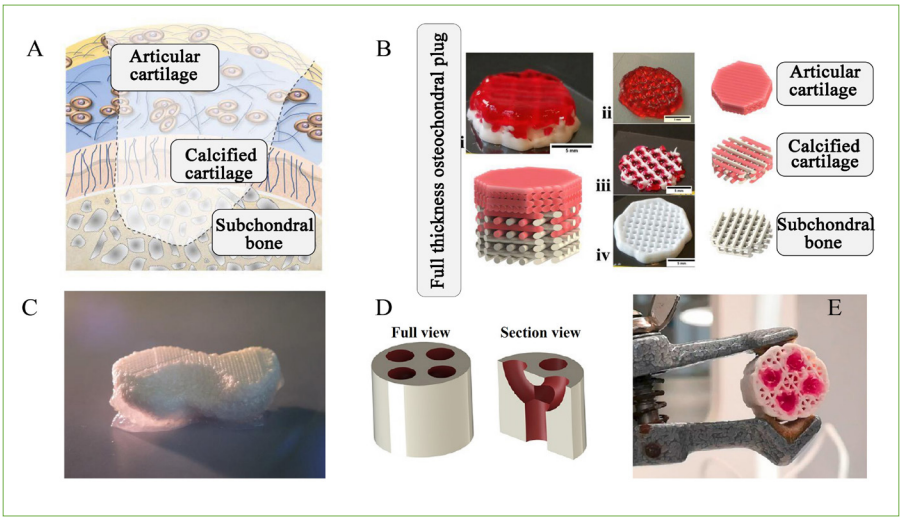

Figure 4. (A) Multi-layered osteochondral tissue defects require zone-specific hierarchical repair strategies. (B) Multi-channel 3D plotting allows the fabrication of artificial full-thickness osteochondral plugs[69]. Image reproduced with permission. (C) 3D multichannel plotting of the scaphoid bone consisting of CPC with mc10 as support ink[62]. Image reproduced with permission. (D) Full and section view of the designed CAD model. The channel branches from one into four channels[70]. (E) The plotted scaffold was manually perfused with undiluted phenol red solution; after perfusion, only the hydrogel was stained, evidencing perfusion through the plotted channel structure[70]. Image reproduced with permission.

Precise temporal and spatial representation of signaling molecules, such as gene complexes, is a considerable challenge for many researchers. Researchers have sought to prepare a gene-activated bio-ink that can be combined with 3D bioprinting to engineer tissue scaffolds that can spatially and temporally control gene expression within the tissues. Gonzalez-Fernandez *et al.* mixed MC with Alg to obtain pore-forming bio-inks loaded with bone marrow MSCs[71]. Using MC as a sacrificial ink, the scaffold could progressively form pores and release chondrogenic molecules (combination of TGF-β3, BMP2, and SOX9) within a controlled range to facilitate early transfection of the encapsulated MSCs *in vivo* and *in vitro*. The addition of MC also improved the printability of the ink and the high fidelity of the scaffold. However, the sacrifice of MC also disrupts the mechanical properties of the scaffold, which may be challenging when grafting into bone defects that are subject to high stress.

3.2. Carboxymethyl cellulose

3.2.1. Physicochemical properties and preparation of carboxymethyl cellulose

Carboxymethyl cellulose (CMC) is a water-soluble cellulose derivative obtained via chemical modification. This modification is performed by replacing the hydroxyl group on the glucopyranose chains of cellulose with carboxymethyl groups (–CH2COOH)[72]. It has a wider range of use than MCs, such as drug administration, biomedical regeneration, textiles, paper, wastewater treatment, and food products. CMC is considered a promising scaffold biomaterial for 3D bioprinting in TE because of its easy chemical modification, good viscosity, shear-thinning, and pH-responsiveness[73]. These characteristics primarily depend on the cellulose source and CMC production method[74]. The transition between sol and gel that occurs with pH changes makes them special pH-responsive hydrogels. CMC has excellent structural and mechanical stability at pH 3–10[75]. When the pH is greater than 10, the hydrogen bonds between CMC molecules are broken, resulting in a sharp decrease in the viscosity of the CMC and loss of mechanical stability; conversely, when pH is less than 3, CMC forms precipitates[76].

CMC is mainly prepared via the Williamson-ether reaction in two steps: alkylation and etherification. CMC can also be formed by generating cellulose triacetate (CTA) intermediates in a mildly acidic medium, followed by *in situ* esterification reactions[72].

3.2.2. CMC 3D bioprinting in cartilage and bone repair

Since the carboxyl group in CMC can act as a nucleation site for calcium ions and improve the biomineralization process, CMC is often combined with other substances to prepare bone scaffolds[77]. CMC, as a negatively charged substance, also plays an important role in TE. Chen *et al.* printed a composite scaffold composed of hydroxyapatite and polymers (gelatin, CS, and CMC)[78]. Positively charged CS and negatively charged CMC can establish powerful electrical interactions to enhance the mechanical properties of the scaffold. The hybrid membrane composed of CS, CMC, and hydroxyapatite exhibited good cell viability and osteocalcin expression and promoted the infiltration of bone tissue *in vivo*[79]. Janarthanan *et al.* added Schiff's

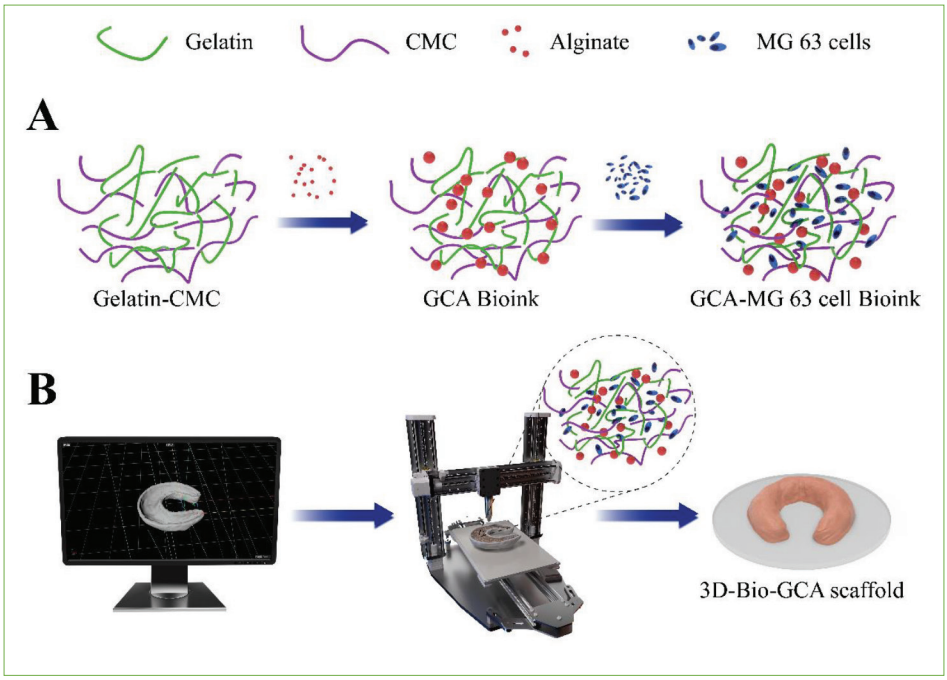

Figure 5. Schematic representation of the preparation of GCA bio-ink and 3D scaffolds. (A) Gelatin-CMC-Alg (GCA) bio-ink loaded with MG 63 osteosarcoma cells. (B) A computer-designed polylactic acid-based meniscus negative mold was printed using 3D printing technology, and then the GCA bio-ink was extruded into the negative mold, and finally demolded to become a 3D-Bio-GCA scaffold.

base reaction[80] to enhance the interaction between CMC and CS and prepared a CMC-glycolic chitosan (GC) 3D printing bio-ink[81]. The aldehyde group of CMC and amine group of GC form an imine bond (C=N) through Schiff's base reaction, and there is also an ionic interaction between the two, which greatly improves the stability of the scaffold. The advantages of this hydrogel scaffold include the lack of any toxic chemical crosslinking agents, fast gel formation (gelation can occur in less than 40 s), and stability of the gel over a range of pH values. Furthermore, lactoferrin was loaded into the hydrogel scaffold, and the loaded bone marrow MSCs showed high activity and a tendency to differentiate. Sathish *et al.*[82] developed a composite trimeric bio-ink comprising gelatin, CMC, and Alg. Additionally, the electrostatic attraction caused by the positive charge of gelatin versus the negative charge of CMC enhances the mechanical characteristics of the material[83]. Simultaneously, creating the bone tissue scaffold was equally creative. The author first used 3D printing technology to make negative meniscal molds from polylactic acid filaments and then extruded composite hydrogel bio-inks loaded with MG63-osteosarcoma cells into the negative meniscal molds (Figure 5). The scaffold exhibited excellent cellular compatibility and proliferation. From day 1 to 7, as the incubation time increased, cellular growth inside the scaffold and collagen secretion from the scaffold increased. This scaffold was created by injecting a cell-loaded bio-ink into a 3D model. This method is effective for preventing cell loss resulting from shearing in conventional 3D bioprinting.

Calcium phosphate has a chemical composition and structure similar to those of bones. However, its use is limited because of its mechanical strength and microporosity. A range of CMC and other cellulose-based additives have been used as binders or gelling agents to maintain cohesion in calcium phosphate formulations[84]. A study by Montelongo *et al.* showed that novel bio-ink formulations with a high β-TCP (75%) to gelatin (25%) ratio are stabilized by the addition of 3% CMC for successful 3D printing of macroporous scaffolds[85]. The scaffold had high porosity and compressive strength, and the 75% TCP+CMC composition promoted early osteogenic commitment and cell adhesion.

Mohan *et al.* fabricated a composite scaffold of NFC and CMC using a combination of direct ink writing (DIW) and freeze-drying (Figure 6)[86]. The scaffolds were obtained using DIW to establish large pores and then using freeze-drying to obtain micropores. Finally, the mechanical properties and wet resilience of the scaffold were further improved via dehydrothermal treatment (DHT). Excellent biocompatibility and high levels of osteoblastic activity were observed on the scaffolds. DHT can not only enhance the hydrogen bond between CMC and NFC to increase the mechanical properties, but also adjust the pore size via water removal. No cellulose degradation was observed

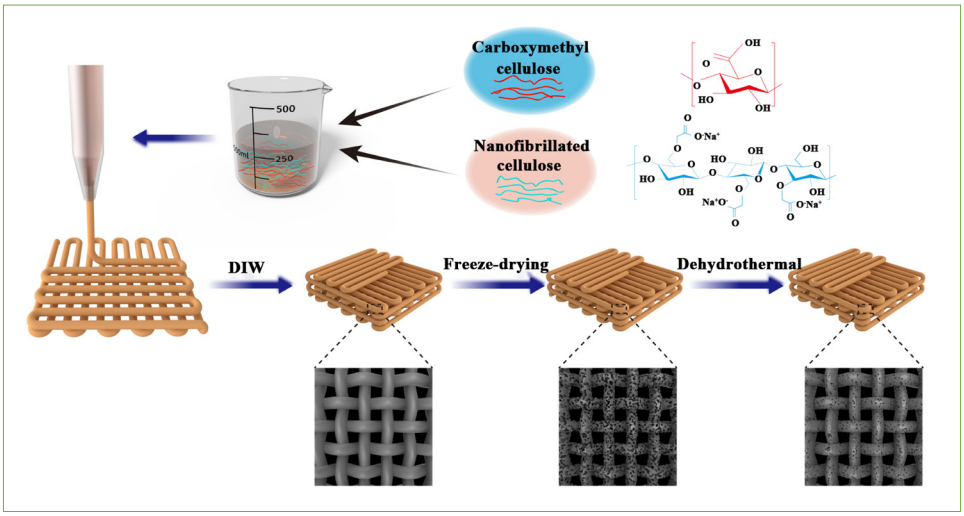

Figure 6. Development of 3D bioscaffolds with macroporous and interconnect microporous morphology from bicomponent ink containing NFC and CMC via the combination of DIW 3D printing, freeze-drying and DHT techniques.

after DHT. Therefore, this technique may inspire pore size adjustment and mechanical property improvement of cellulose-based scaffolds.

3.3 Hydroxypropyl methylcellulose

Hydroxypropyl methylcellulose (HPMC) is also a cellulose ether derivative; however, it is available in different substitution types with limits on methoxy and hydroxypropoxy groups[87]. These groups provide various characteristics, including flexibility, hydration, gelation temperature, and LCST behavior. Moreover, in medical engineering, HPMC is mainly used as a material for encapsulating drugs[88] or as an ink tackifier in TE scaffolds[89]. Götz *et al.* prepared degradable bone implants using extrusion-based 3D printing with HPMC and calcium magnesium phosphate polymers[89]. The addition of HPMC increased the viscosity and shear-thinning behavior of the ink. Ni *et al.* integrated SF and HPMC for printing a bone marrow MSCs-laden DN hydrogel for cartilage tissue repair[90]. The β-sheet structure between SF molecules is formed via low-power ultrasonication of SF and acts as the rigid first network, whereas the HPMC-methacrylate anhydride (MAn) crosslink acts as the soft second network. HPMC modified with MA forms a tight bond between SF and HPMC-MAn because of the exposure of more hydrogen bonds that interact with the β-sheet. Simultaneously, the presence of HPMC has a synergistic effect on the gelation of SF[91]. This DN hydrogel combines the advantages of the two different hydrogels and has good mechanical properties[92]. Moreover, loaded bone marrow MSCs have high activity and proliferative tendencies. At the same time, high expression of cartilage-related genes, such as high mobility group-box gene9 (*Sox 9*) and collagen type II (*Col II*), was detected.

3.4. HEC

Owing to its excellent shear-thinning behavior and outstanding rheological properties[93], along with its biocompatibility, HEC is often used as an additive in bioengineered inks to meet the bioprinting requirements. Li *et al.* added HEC to several bio-inks with different crosslinks to evaluate its effects on the fidelity, degradation, and rheology of bio-inks[94]. The results show that HEC can improve the fidelity of these bio-inks without affecting their crosslinks. In addition, HEC improves the LCST of the gel, enabling 3D bioprinting at near body temperature. HEC increases the swelling rate to ensure a water-rich environment in the scaffold for increased cell activity and nutrient delivery. Therefore, HEC can be used to modify bio-inks in several ways. Maturavongsadit *et al.* prepared cell-laden nanocellulose/CS-based bio-inks for 3D bioprinting[31]. The authors added HEC as a gelling agent to the CS-NCC bio-ink to improve its gelation kinetics. The glyoxal groups in HEC interact with the amine group of CS via covalent crosslinking through the Schiff's base reaction[95]. With the addition of HEC, the gelation time of this hydrogel was significantly reduced without affecting the biocompatibility of the 3D-bioprinted bone tissue scaffold.

4. Conclusion and outlook

In this review, we focus on the applications of nanocellulose and cellulose derivatives in 3D bioprinting for bone and cartilage TE. As it meets the basic requirements of bio-inks and is easily modified, nanocellulose has been widely used in 3D printing. T-NFC modified by TEMPO oxidation has a good nucleation effect on hydroxyapatite and is suitable for bone TE, while the anionic carboxylic acid group in T-NFC can form ionic crosslinks with cations to enhance the mechanical

properties of the scaffold. NCC has the best tensile strength because it contains only crystalline regions, and is often used as a key element for improving the mechanical properties of scaffolds. BNC has the highest water content and strongest water absorption capacity for cell survival, as well as a porous nanofiber mesh structure that promotes cell adhesion, and is quite popular in 3D bioprinting. Particularly, BNC can be used as a pore size modifier for TE with different pore size requirements[96,97]. *In situ* and *ex situ* BNC modifications are well established. However, preparing well-dispersed BNC and eliminating potential endotoxins from bacteria is laborious and expensive.

Cellulose derivatives also meet the basic requirements of bio-inks and have certain advantages. MC is often cleared for final processing into complex or porous structures during TE scaffold preparation because of its biological inertness and its characteristics as a temperature-responsive polymer. The carboxyl group in CMC can act as a nucleation site for calcium ions to improve bone mineralization. As a negatively charged polymer, it can form strong electrical interactions with positively charged polymers (e.g., CS and gelatin) to improve the fidelity of the scaffold, which is important in bone TE.

Nanocellulose and cellulose derivatives are promising candidates for the development of biologically fabricated structures. However, there is currently relatively little *in vivo* clinical evidence in this area. Also, their potential in this area has not yet been fully realized. For example, the temperature responsiveness of MCs or the pH responsiveness of CMCs can be exploited to prepare stimuli-responsive hydrogels suitable for 3D bioprinting. Inspired by the NCC and NFC mixed ink, the use of BNC and NCC or NFC to prepare mixed ink can be exploited in their respective emerging fields. We hope that this review will inspire researchers to design novel bio-inks based on cellulose and its derivatives for use in bone and cartilage TE.

Acknowledgments

Not applicable.

Funding

This work was supported by grants from the National Natural Science Foundation of China (No. 81871775), Zhejiang Provincial Natural Science Foundation of China (No. LBY21H060001, LGF21H060002), and Medical and Health Research Project of Zhejiang Province (NO. 2020RC115, 2020KY929).

Conflict of interest

The authors declare no conflicts of interest.

Author contributions

Conceptualization: Lei Zhang, Guojing Yang
Writing – original draft: Lan Lin, Songli Jiang
Writing – review & editing: Jiandi Qiu, Jun Yang, Xiaoyi Jiao, Xusong Yue, Xiurong Ke
All authors agree and approve the manuscript for publication.

Ethics approval and consent to participate

Not applicable.

Consent for publication

Not applicable.

Availability of data

Not applicable.

References

1. Zhang YS, Yue K, Aleman J, *et al.*, 2017, 3D bioprinting for tissue and organ fabrication. *Ann Biomed Eng*, 45: 148–163.

https://doi.org/10.1007/s10439-016-1612-8

2. Mota C, Camarero-Espinosa S, Baker MB, *et al.*, 2020, Bioprinting: from tissue and organ development to in vitro models. *Chem Rev*, 120: 10547–10607.

https://doi.org/10.1021/acs.chemrev.9b00789

3. Tarassoli SP, Jessop ZM, Al-Sabah A, *et al.*, 2018, Skin tissue engineering using 3D bioprinting: An evolving research field. *J Plast Reconst Aesthet Surg*, 71: 615–623.

https://doi.org/10.1016/j.bjps.2017.12.006

4. Alonzo M, AnilKumar S, Roman B, *et al.*, 2019, 3D Bioprinting of cardiac tissue and cardiac stem cell therapy. *Transl Res*, 211: 64–83.

https://doi.org/10.1016/j.trsl.2019.04.004

5. Mei Q, Rao J, Bei HP, *et al.*, 2021, 3D bioprinting photo-crosslinkable hydrogels for bone and cartilage repair. *Int J Bioprinting*, 7: 367.

https://doi.org/10.18063/ijb.v7i3.367

6. Heinrich MA, Liu W, Jimenez A, *et al.*, 2019, 3D Bioprinting: from benches to translational applications. *Small*, 15: e1805510.

https://doi.org/10.1002/smll.201805510

7. Thomas P, Duolikun T, Rumjit NP, *et al.*, 2020, Comprehensive review on nanocellulose: Recent developments, challenges and future prospects. *J Mech Behav Biomed Mater*, 110: 103884.

https://doi.org/10.1016/j.jmbbm.2020.103884

8. Piras CC, Fernández-Prieto S, De Borggraeve WM, 2017, Nanocellulosic materials as bioinks for 3D bioprinting. *Biomater Sci*, 5: 1988–1992.

   https://doi.org/10.1039/c7bm00510e

9. Banvillet G, Depres G, Belgacem N, *et al.*, 2021, Alkaline treatment combined with enzymatic hydrolysis for efficient cellulose nanofibrils production. *Carbohydr Polym*, 255: 117383. \

   https://doi.org/10.1016/j.carbpol.2020.117383

10. Isogai A, Saito T, Fukuzumi H, 2011, TEMPO-oxidized cellulose nanofibers. *Nanoscale*, 3: 71–85.

    https://doi.org/10.1039/c0nr00583e

11. Piras CC, Fernandez-Prieto S, De Borggraeve WM, 2017, Nanocellulosic materials as bioinks for 3D bioprinting. *Biomater Sci*, 5: 1988–1992.

    https://doi.org/10.1039/c7bm00510e

12. Starborg T, Kalson NS, Lu Y, *et al.*, 2013, Using transmission electron microscopy and 3View to determine collagen fibril size and three-dimensional organization. *Nat Protoc*, 8: 1433–1448.

    https://doi.org/10.1038/nprot.2013.086

13. Rouillard AD, Berglund CM, Lee JY, *et al.*, 2011, Methods for photocrosslinking alginate hydrogel scaffolds with high cell viability. *Tissue Eng C: Methods*, 17: 173–179.

    https://doi.org/10.1089/ten.TEC.2009.0582

14. Markstedt K, Mantas A, Tournier I, *et al.*, 2015, 3D bioprinting human chondrocytes with nanocellulose-alginate bioink for cartilage tissue engineering applications. *Biomacromolecules*, 16: 1489–1496.

    https://doi.org/10.1021/acs.biomac.5b00188

15. Trachsel L, Johnbosco C, Lang T, *et al.*, 2019, Double-network hydrogels including enzymatically crosslinked Poly-(2-alkyl-2-oxazoline)s for 3D bioprinting of cartilage-engineering constructs. *Biomacromolecules*, 20: 4502–4511.

    https://doi.org/10.1021/acs.biomac.9b01266

16. Yasuda K, Ping Gong J, Katsuyama Y, *et al.*, 2005, Biomechanical properties of high-toughness double network hydrogels. *Biomaterials*, 26: 4468–4475.

    https://doi.org/10.1016/j.biomaterials.2004.11.021

17. Öztürk E, Arlov Ø, Aksel S, *et al.*, 2016, Sulfated hydrogel matrices direct mitogenicity and maintenance of chondrocyte phenotype through activation of FGF signaling. *Adv Funct Mater*, 26: 3649–3662.

    https://doi.org/10.1002/adfm.201600092

18. Müller M, Öztürk E, Arlov Ø, *et al.*, 2017, Alginate Sulfate-nanocellulose bioinks for cartilage bioprinting applications. *Ann Biomed Eng*, 45: 210–223.

    https://doi.org/10.1007/s10439-016-1704-5

19. Apelgren P, Amoroso M, Lindahl A, *et al.*, 2017, Chondrocytes and stem cells in 3D-bioprinted structures create human cartilage in vivo. *PloS One*, 12: e0189428.

    https://doi.org/10.1371/journal.pone.0189428

20. Morimune-Moriya S, Kondo S, Sugawara-Narutaki A, *et al.*, 2014, Hydroxyapatite formation on oxidized cellulose nanofibers in a solution mimicking body fluid. *Polym J*, 47: 158–163.

    https://doi.org/10.1038/pj.2014.127

21. Abouzeid RE, Khiari R, Beneventi D, *et al.*, 2018, Biomimetic mineralization of three-dimensional printed Alginate/TEMPO-Oxidized cellulose nanofibril scaffolds for bone tissue engineering. *Biomacromolecules*, 19: 4442–4452.

    https://doi.org/10.1021/acs.biomac.8b01325

22. Im S, Choe G, Seok JM, *et al.*, 2022, An osteogenic bioink composed of alginate, cellulose nanofibrils, and polydopamine nanoparticles for 3D bioprinting and bone tissue engineering. *Int J Biol Macromol*, 205: 520–529.

    https://doi.org/10.1016/j.ijbiomac.2022.02.012

23. Ojansivu M, Vanhatupa S, Björkvik L, *et al.*, 2015, Bioactive glass ions as strong enhancers of osteogenic differentiation in human adipose stem cells. *Acta Biomater*, 21: 190–203.

    https://doi.org/10.1016/j.actbio.2015.04.017

24. Ojansivu M, Rashad A, Ahlinder A, *et al.*, 2019, Wood-based nanocellulose and bioactive glass modified gelatin-alginate bioinks for 3D bioprinting of bone cells. *Biofabrication*, 11: 035010.

    https://doi.org/10.1088/1758-5090/ab0692

25. Monfared M, Mawad D, Rnjak-Kovacina J, *et al.*, 2021,3D bioprinting of dual-crosslinked nanocellulose hydrogels for tissue engineering applications. *J Mater Chem B*, 9: 6163–6175.

    https://doi.org/10.1039/d1tb00624j

26. Mtibe A, Linganiso LZ, Mathew AP, *et al.*, 2015, A comparative study on properties of micro and nanopapers produced from cellulose and cellulose nanofibres. *Carbohydr Polym*, 118: 1–8.

    https://doi.org/10.1016/j.carbpol.2014.10.007

27. Karimian A, Parsian H, Majidinia M, *et al.*, 2019, Nanocrystalline cellulose: Preparation, physicochemical properties, and applications in drug delivery systems. *Int J Biol Macromol*, 133: 850–859.

    https://doi.org/10.1016/j.ijbiomac.2019.04.117

28. Murizan NIS, Mustafa NS, Ngadiman NHA, *et al.*, 2020, Review on nanocrystalline cellulose in bone tissue engineering applications. *Polymers*, 12: 2818.

    https://doi.org/10.3390/polym12122818

29. Osorio DA, Lee BEJ, Kwiecien JM, *et al.*, 2019, Cross-linked cellulose nanocrystal aerogels as viable bone tissue scaffolds. *Acta Biomater*, 87: 152–165.

https://doi.org/10.1016/j.actbio.2019.01.049

30. Wang K, Nune KC, Misra RD, 2016, The functional response of alginate-gelatin-nanocrystalline cellulose injectable hydrogels toward delivery of cells and bioactive molecules. *Acta Biomater*, 36: 143–151.

https://doi.org/10.1016/j.actbio.2016.03.016

31. Maturavongsadit P, Narayanan LK, Chansoria P, *et al.*, 2021, Cell-laden nanocellulose/chitosan-based bioinks for 3D bioprinting and enhanced osteogenic cell differentiation. *ACS Appl Bio Mater*, 4: 2342–2353.

https://doi.org/10.1021/acsabm.0c01108

32. Murphy WL, McDevitt TC, Engler AJ, 2014, Materials as stem cell regulators. *Nat Mater*, 13: 547–557.

https://doi.org/10.1038/nmat3937

33. Dutta SD, Hexiu J, Patel DK, *et al.*, 2021, 3D-printed bioactive and biodegradable hydrogel scaffolds of alginate/gelatin/cellulose nanocrystals for tissue engineering. *Int J Biol Macromol*, 167: 644–658.

https://doi.org/10.1016/j.ijbiomac.2020.12.011

34. Patel DK, Dutta SD, Shin WC, *et al.*, 2021, Fabrication and characterization of 3D printable nanocellulose-based hydrogels for tissue engineering. *RSC Adv*, 11: 7466–7478.

https://doi.org/10.1039/d0ra09620b

35. Hosseinidoust Z, Alam MN, Sim G, *et al.*, 2015, Cellulose nanocrystals with tunable surface charge for nanomedicine. *Nanoscale*, 7: 16647–16657.

https://doi.org/10.1039/c5nr02506k

36. Nelson KIM, Retsina T, 2014, Innovative nanocellulose process breaks the cost barrier. *TAPPI J*, 13: 19–23.

https://doi.org/10.32964/tj13.5.19

37. Jessop ZM, Al-Sabah A, Gao N, *et al.*, 2019, Printability of pulp derived crystal, fibril and blend nanocellulose-alginate bioinks for extrusion 3D bioprinting. *Biofabrication*, 11: 045006.

https://doi.org/10.1088/1758-5090/ab0631

38. Barna M, Niswander L, 2007, Visualization of cartilage formation: insight into cellular properties of skeletal progenitors and chondrodysplasia syndromes. *Dev Cell*, 12: 931–941.

https://doi.org/10.1016/j.devcel.2007.04.016

39. Williams WS, Cannon RE, 1989, Alternative environmental roles for cellulose produced by acetobacter xylinum. *Appl Environ Microbiol*, 55: 2448–2452.

https://doi.org/10.1128/aem.55.10.2448-2452.1989

40. Dugan JM, Gough JE, Eichhorn SJ, 2013, Bacterial cellulose scaffolds and cellulose nanowhiskers for tissue engineering. *Nanomedicine Lond*, 8: 287–298.

https://doi.org/10.2217/nnm.12.211

41. Swingler S, Gupta A, Gibson H, *et al.*, 2021, Recent advances and applications of bacterial cellulose in biomedicine. *Polymers*, 13: 412.

https://doi.org/10.3390/polym13030412

42. Salgado L, Blank S, Esfahani RAM, *et al.*, 2019, Missense mutations in a transmembrane domain of the Komagataeibacter xylinus BcsA lead to changes in cellulose synthesis. *BMC Microbiol*, 19: 216.

https://doi.org/10.1186/s12866-019-1577-5

43. Ishikawa A, Matsuoka M, Tsuchida T, *et al.*, 2014, Increase in cellulose production by sulfaguanidine-resistant mutants derived fromacetobacter xylinumsubsp.sucrofermentans. *Biosci Biotechnol Biochem*, 59: 2259–2262.

https://doi.org/10.1271/bbb.59.2259

44. Stumpf TR, Yang X, Zhang J, *et al.*, 2018, In situ and ex situ modifications of bacterial cellulose for applications in tissue engineering. *Mat Sci Eng C, Mater biol Appl*, 82: 372–383.

https://doi.org/10.1016/j.msec.2016.11.121

45. Zaborowska M, Bodin A, Bäckdahl H, *et al.*, 2010, Microporous bacterial cellulose as a potential scaffold for bone regeneration. *Acta Biomater*, 6: 2540–2547.

https://doi.org/10.1016/j.actbio.2010.01.004

46. Fang B, Wan YZ, Tang TT, *et al.*, 2009, Proliferation and osteoblastic differentiation of human bone marrow stromal cells on hydroxyapatite/bacterial cellulose nanocomposite scaffolds. *Tissue Eng Part A*, 15: 1091–1098.

https://doi.org/10.1089/ten.tea.2008.0110

47. Krontiras P, Gatenholm P, Hägg DA, 2015, Adipogenic differentiation of stem cells in three-dimensional porous bacterial nanocellulose scaffolds. *J Biomed Mater Res Part B, Appl biomater*, 103: 195–203.

https://doi.org/10.1002/jbm.b.33198

48. Bian H, Chen L, Dai H, *et al.*, 2017, Integrated production of lignin containing cellulose nanocrystals (LCNC) and nanofibrils (LCNF) using an easily recyclable di-carboxylic acid. *Carbohydr Polym*, 167: 167–176.

https://doi.org/10.1016/j.carbpol.2017.03.050

49. Wang X, Tang S, Chai S, *et al.*, 2021, Preparing printable bacterial cellulose based gelatin gel to promote in vivo bone regeneration. *Carbohydr Polym*, 270: 118342.

https://doi.org/10.1016/j.carbpol.2021.118342

50. Kondo T, Kose R, Naito H, *et al.*, 2014, Aqueous counter collision using paired water jets as a novel means of preparing bio-nanofibers. *Carbohydr Polym*, 112: 284–290.

https://doi.org/10.1016/j.carbpol.2014.05.064

51. Apelgren P, Karabulut E, Amoroso M, *et al.*, 2019, In vivo human cartilage formation in three-dimensional bioprinted constructs with a novel bacterial nanocellulose bioink. *ACS Biomater Sci Eng*, 5: 2482–2490.

https://doi.org/10.1021/acsbiomaterials.9b00157

52. Huang L, Du X, Fan S, *et al.*, 2019, Bacterial cellulose nanofibers promote stress and fidelity of 3D-printed silk based hydrogel scaffold with hierarchical pores. *Carbohydr polym*, 221: 146–156.

https://doi.org/10.1016/j.carbpol.2019.05.080

53. Matsiko A, Gleeson JP, O'Brien FJ, 2015, Scaffold mean pore size influences mesenchymal stem cell chondrogenic differentiation and matrix deposition. *Tissue Eng Part A*, 21: 486–497.

https://doi.org/10.1089/ten.TEA.2013.0545

54. Arca HC, Mosquera-Giraldo LI, Bi V, *et al.*, 2018, Pharmaceutical Applications of Cellulose Ethers and Cellulose Ether Esters. *Biomacromolecules*, 19: 2351–2376.

https://doi.org/10.1021/acs.biomac.8b00517

55. Ratanakamnuan U, Atong D, Aht-Ong D, 2012, Cellulose esters from waste cotton fabric via conventional and microwave heating. *Carbohydr Polym*, 87: 84–94.

https://doi.org/10.1016/j.carbpol.2011.07.016

56. Yang J, An X, Liu L, *et al.*, 2020, Cellulose, hemicellulose, lignin, and their derivatives as multi-components of bio-based feedstocks for 3D printing. *Carbohydr Polym*, 250: 116881.

https://doi.org/10.1016/j.carbpol.2020.116881

57. Ahlfeld T, Guduric V, Duin S, *et al.*, 2020, Methylcellulose – a versatile printing material that enables biofabrication of tissue equivalents with high shape fidelity. *Biomater Sci*, 8: 2102–2110.

https://doi.org/10.1039/d0bm00027b

58. Bonetti L, De Nardo L, Farè S, 2021, Thermo-responsive methylcellulose hydrogels: from design to applications as smart biomaterials. *Tissue Eng Part B, Rev*, 27: 486–513.

https://doi.org/10.1089/ten.TEB.2020.0202

59. Nasatto P, Pignon F, Silveira J, *et al.*, 2015, Methylcellulose, a cellulose derivative with original physical properties and extended applications. *Polymers*, 7: 777–803.

https://doi.org/10.3390/polym7050777

60. Kim MH, Kim BS, Park H, *et al.*, 2018, Injectable methylcellulose hydrogel containing calcium phosphate nanoparticles for bone regeneration. *Int J Biol Macromol*, 109: 57–64.

https://doi.org/10.1016/j.ijbiomac.2017.12.068

61. Altomare L, Bonetti L, Campiglio CE, *et al.*, 2018, Biopolymer-based strategies in the design of smart medical devices and artificial organs. *Int J Artif Organs*, 41: 337–359.

https://doi.org/10.1177/0391398818765323

62. Ahlfeld T, Köhler T, Czichy C, *et al.*, 2018, A methylcellulose hydrogel as support for 3D plotting of complex shaped calcium phosphate scaffolds. *Gels (Basel, Switzerland)*, 4: 68.

https://doi.org/10.3390/gels4030068

63. Hodder E, Duin S, Kilian D, *et al.*, 2019, Investigating the effect of sterilisation methods on the physical properties and cytocompatibility of methyl cellulose used in combination with alginate for 3D-bioplotting of chondrocytes. *J Mater Scimater Med*, 30: 10.

https://doi.org/10.1007/s10856-018-6211-9

64. Ke H, Zhou J, Zhang L, 2006, Structure and physical properties of methylcellulose synthesized in NaOH/urea solution. *Polym Bull*, 56: 349–357.

https://doi.org/10.1007/s00289-006-0507-5

65. de Carvalho Oliveira G, Filho GR, Vieira JG, *et al.*, 2010, Synthesis and application of methylcellulose extracted from waste newspaper in CPV-ARI Portland cement mortars. *J Appl Poly Sci*, 118: 1380–1385.

https://doi.org/10.1002/app.32477

66. Schütz K, Placht AM, Paul B, *et al.*, 2017, Three-dimensional plotting of a cell-laden alginate/methylcellulose blend: towards biofabrication of tissue engineering constructs with clinically relevant dimensions. *J Tissue Engregen Med*, 11: 1574–1587.

https://doi.org/10.1002/term.2058

67. Ahlfeld T, Doberenz F, Kilian D, *et al.*, 2018, Bioprinting of mineralized constructs utilizing multichannel plotting of a self-setting calcium phosphate cement and a cell-laden bioink. *Biofabrication*, 10: 045002.

https://doi.org/10.1088/1758-5090/aad36d

68. Bernhardt A, Schumacher M, Gelinsky M, 2015, Formation of osteoclasts on calcium phosphate bone cements and polystyrene depends on monocyte isolation conditions. *Tissue Eng Part C, Methods*, 21: 160–170.

https://doi.org/10.1089/ten.TEC.2014.0187

69. Kilian D, Ahlfeld T, Akkineni AR *et al*, 2020, 3D Bioprinting of osteochondral tissue substitutes – in vitro-chondrogenesis in multi-layered mineralized constructs. *Sci Rep*, 10: 8277.

https://doi.org/10.1038/s41598-020-65050-9

70. Ahlfeld T, Cubo-Mateo N, Cometta S, *et al.*, 2020, A novel plasma-based bioink stimulates cell proliferation and differentiation in bioprinted, mineralized constructs. *ACS Appl Mater Interfaces*, 12: 12557–12572.

https://doi.org/10.1021/acsami.0c00710

71. Gonzalez-Fernandez T, Rathan S, Hobbs C, *et al.*, 2019, Pore-forming bioinks to enable spatio-temporally defined gene delivery in bioprinted tissues. *JCR*, 301: 13–27.

https://doi.org/10.1016/j.jconrel.2019.03.006

72. Rahman MS, Hasan MS, Nitai AS, *et al.*, 2021, Recent developments of carboxymethyl cellulose. *Polymers*, 13: 1345.

https://doi.org/10.3390/polym13081345

73. Zennifer A, Senthilvelan P, Sethuraman S, *et al.*, 2021, Key advances of carboxymethyl cellulose in tissue engineering & 3D bioprinting applications. *Carbohydr Poly*, 256: 117561.

https://doi.org/10.1016/j.carbpol.2020.117561

74. Rachtanapun P, Jantrawut P, Klunklin W, *et al.*, 2021, Carboxymethyl bacterial cellulose from nata de coco: effects of NaOH. *Polymers*, 13: 348.

https://doi.org/10.3390/polym13030348

75. Gaihre B, Jayasuriya AC, 2016, Fabrication and characterization of carboxymethyl cellulose novel microparticles for bone tissue engineering. *Mater Sci Eng C Mater Biol Appl*, 69: 733–743.

https://doi.org/10.1016/j.msec.2016.07.060

76. Mallakpour S, Tukhani M, Hussain CM, 2021, Recent advancements in 3D bioprinting technology of carboxymethyl cellulose-based hydrogels: Utilization in tissue engineering. *Adv Colloid Interface Sci*, 292: 102415.

https://doi.org/10.1016/j.cis.2021.102415

77. Singh BN, Panda NN, Mund R, *et al.*, 2016, Carboxymethyl cellulose enables silk fibroin nanofibrous scaffold with enhanced biomimetic potential for bone tissue engineering application. *Carbohydr Poly*, 151: 335–347.

https://doi.org/10.1016/j.carbpol.2016.05.088

78. Chen S, Shi Y, Zhang X, *et al.*, 2019, 3D printed hydroxyapatite composite scaffolds with enhanced mechanical properties. *Ceram Int*, 45: 10991–10996.

https://doi.org/10.1016/j.ceramint.2019.02.182

79. Jiang H, Zuo Y, Zou Q, *et al.*, 2013, Biomimetic spiral-cylindrical scaffold based on hybrid chitosan/cellulose/nano-hydroxyapatite membrane for bone regeneration. *ACS App Mater Interfaces*, 5: 12036–12044.

https://doi.org/10.1021/am4038432

80. Resmi R, Parvathy J, John A, *et al.*, 2020, Injectable self-crosslinking hydrogels for meniscal repair: A study with oxidized alginate and gelatin. *Carbohydr Poly*, 234: 115902.

https://doi.org/10.1016/j.carbpol.2020.115902

81. Janarthanan G, Tran HN, Cha E, *et al.*, 2020,3D printable and injectable lactoferrin-loaded carboxymethyl cellulose-glycol chitosan hydrogels for tissue engineering applications. *Mat Sci Eng*, 113: 111008.

https://doi.org/10.1016/j.msec.2020.111008

82. P BS, S G, J P, *et al.*, 2022, Tricomposite gelatin-carboxymethylcellulose-alginate bioink for direct and indirect 3D printing of human knee meniscal scaffold. *Intbiol Macromol*, 195: 179–189.

https://doi.org/10.1016/j.ijbiomac.2021.11.184

83. Duhoranimana E, Karangwa E, Lai L, *et al.*, 2017, Effect of sodium carboxymethyl cellulose on complex coacervates formation with gelatin: Coacervates characterization, stabilization and formation mechanism. *Food Hydrocoll*, 69: 111–120.

https://doi.org/10.1016/j.foodhyd.2017.01.035

84. Kobayashi H, Fujishiro T, Belkoff SM, *et al.*, 2009, Long-term evaluation of a calcium phosphate bone cement with carboxymethyl cellulose in a vertebral defect model. *J Biomedmater Res A*, 88: 880–888.

https://doi.org/10.1002/jbm.a.31933

85. Montelongo SA, Chiou G, Ong JL, *et al.*, 2021, Development of bioinks for 3D printing microporous, sintered calcium phosphate scaffolds. *J Mater Sci Mater Med*, 32: 94.

https://doi.org/10.1007/s10856-021-06569-9

86. Mohan T, Dobaj Štiglic A, Beaumont M, *et al.*, 2020, Generic method for designing self-standing and dual porous 3d bioscaffolds from cellulosic nanomaterials for tissue engineering applications. *ACS Appl Bio Mater*, 3: 1197–1209.

https://doi.org/10.1021/acsabm.9b01099

87. Al-Tabakha MM, 2010, HPMC capsules: current status and future prospects. *JPPS*, 13: 428–442.

https://doi.org/10.18433/j3k881

88. Koehl NJ, Shah S, Tenekam ID, *et al.*, 2021, Lipid based formulations in hard gelatin and hpmc capsules: a physical compatibility study. *Pharm Res*, 38: 1439–1454.

https://doi.org/10.1007/s11095-021-03088-8

89. Götz LM, Holeczek K, Groll J, *et al.*, 2021, Extrusion-based 3D printing of calcium magnesium phosphate cement pastes for degradable bone implants. *Materials (Basel, Switzerland)*, 14: 5197.

https://doi.org/10.3390/ma14185197

90. Ni T, Liu M, Zhang Y, *et al.*, 2020, 3D Bioprinting of bone marrow mesenchymal stem cell-laden silk fibroin double network scaffolds for cartilage tissue repair. *Bioconjug Chem*, 31: 1938–1947.

https://doi.org/10.1021/acs.bioconjchem.0c00298

91. Luo K, Yang Y, Shao Z, 2016, Physically crosslinked biocompatible silk-fibroin-based hydrogels with high mechanical performance. *Adv Funct Mater*, 26: 872–880.

https://doi.org/10.1002/adfm.201503450

92. Gong JP, 2010, Why are double network hydrogels so tough? *Soft Matter*, 6: 2583–2590.

https://doi.org/10.1039/b924290b

93. Maestro A, González C, Gutiérrez JM, 2002, Shear thinning and thixotropy of HMHEC and HEC water solutions. *J Rheol*, 46: 1445–1457.

https://doi.org/10.1122/1.1516789

94. Li X, Deng Q, Wang S, *et al.*, 2021, Hydroxyethyl cellulose as a rheological additive for tuning the extrusion printability and scaffold properties. *3D Prin Add Man*, 8: 87–98.

https://doi.org/10.1089/3dp.2020.0167

95. Maturavongsadit P, Paravyan G, Shrivastava R, *et al.*, 2020, Thermo-/pH-responsive chitosan-cellulose nanocrystals based hydrogel with tunable mechanical properties for tissue regeneration applications. *Mater*, 12: 100681.

https://doi.org/10.1016/j.mtla.2020.100681

96. Cakmak AM, Unal S, Sahin A, *et al.*, 2020, 3D printed polycaprolactone/gelatin/bacterial cellulose/hydroxyapatite composite scaffold for bone tissue engineering. *Poly*, 12: 1962.

https://doi.org/10.3390/polym12091962

97. Aki D, Ulag S, Unal S, *et al.*, 2020, 3D printing of PVA/hexagonal boron nitride/bacterial cellulose composite scaffolds for bone tissue engineering. *Mater Des*, 196: 109094.

https://doi.org/10.1016/j.matdes.2020.109094